

# Wavelength tunable passively $Q$ -switched Yb-doped double-clad fiber laser with graphene grown on SiC

Liqiang Zhang (张丽强)<sup>1</sup>, Zhuang Zhuo (卓 壮)<sup>1\*</sup>, Rusheng Wei (魏汝省)<sup>2</sup>,  
Yunzheng Wang (王云征)<sup>1</sup>, Xiufang Chen (陈秀芳)<sup>2</sup>, and Xiangang Xu (徐现刚)<sup>2</sup>

<sup>1</sup>School of Information Science and Engineering, Shandong University, Jinan 250100, China

<sup>2</sup>State Key Laboratory of Crystal Material, Shandong University, Jinan 250100, China

\*Corresponding author: zhuozhuang@sdu.edu.cn

Received September 29, 2013; accepted December 20, 2013; posted online January 27, 2014

A passively  $Q$ -switched tunable Yb-doped double-clad fiber laser is demonstrated with graphene epitaxially grown on SiC. The spectral tuning of the  $Q$ -switched fiber laser is implemented by rotating a quartz plate filter inside the cavity. The central wavelength of the fiber laser can be continuously tuned from 1038.54 to 1056.22 nm. The maximum pulse energy of 0.65  $\mu$ J is obtained at the pump power of 4.08 W, and the corresponding pulse duration and average output power are 1.60  $\mu$ s and 35 mW, respectively.

OCIS codes: 140.3540, 140.3510, 140.3600, 140.3538.

doi: 10.3788/COL201412.021405.

$Q$ -switched fiber lasers are of great interest in recent years because of their intensive applications in rang finding, remote sensing, medicine and so on<sup>[1–3]</sup>. Compared with actively  $Q$ -switched fiber lasers, passive ones possess the attractive advantages of simplicity, low cost, flexibility and so on. Passively  $Q$ -switched fiber lasers have been demonstrated with different kinds of saturable absorbers, including metal-doped bulk crystals<sup>[4,5]</sup>, semiconductor saturable absorber mirrors<sup>[6]</sup>, carbon nanotubes<sup>[7,8]</sup>, and graphene<sup>[9–13]</sup>. Among of them, graphene has been paid increasing attention since it was obtained in 2004. Unlike conventional semiconductor saturable absorbers, the energy band diagram of graphene has zero band gap and a linear dispersion relation. These unique energy band properties combined with the Pauli blocking principle render graphene a full band saturable absorber<sup>[14]</sup>, which is extremely suitable for tunable  $Q$ -switched/mode-locked lasers. Moreover, graphene has the advantages of ultrafast carrier dynamics, low cost, controllable modulation depth and so on<sup>[15]</sup>.

A number of research groups worldwide have demonstrated applications of graphene as saturable absorbers in pulsed fiber lasers. Graphene  $Q$ -switched fiber lasers was demonstrated by Luo *et al.* in 2010<sup>[16]</sup>. To exploit the wideband saturable absorption, passively  $Q$ -switched fiber lasers at different wavelengths<sup>[17–23]</sup> and graphene  $Q$ -switched tunable fiber lasers<sup>[24–27]</sup> were investigated. However, all of the tunable  $Q$ -switched fiber lasers based on graphene were obtained around 1.5  $\mu$ m.

The common method to implement a compact graphene mode-locked/ $Q$ -switched fiber laser system is to sandwich a piece of graphene film between two fiber connectors with a fiber adaptor. However, this method easily leads to the damage of the saturable absorber due to the large thermal deposition in the graphene. In addition, the fabrication of these graphene-based saturable absorbers requires a complex transferring process. Graphene epitaxially grown on SiC provides an alternative solution. Graphene-on-SiC could be inserted in the cavity with the substrate directly without trans-

ferring process. In addition, the SiC substrate could also play the role of heat-sink to reduce the thermal effect arisen from the absorbing of the laser during the switching<sup>[28]</sup>. In 2010, Yu *et al.*<sup>[28]</sup> demonstrated a large energy neodymium-doped yttrium aluminum garnet crystal laser  $Q$ -switched by graphene grown on SiC. Recently, Men *et al.*<sup>[29]</sup> reported a graphene passively  $Q$ -switched Nd:YAG ceramic laser at 1123 nm.

In this letter, a wavelength tunable Yb-doped double-clad fiber laser was demonstrated. Graphene epitaxially grown on SiC was used as the saturable absorber, and a wavelength tuning range of  $\sim 18$  nm was obtained.

Graphene used in our experiment was epitaxially grown on SiC. The number of graphene layers was round 10. Figure 1 gives the measured Raman spectrum of the graphene. The prominent G and 2D peaks are located at 1583 and 2702  $\text{cm}^{-1}$ . The FWHMs are 19 and 33  $\text{cm}^{-1}$ , respectively. The relatively weak D peak at 1357  $\text{cm}^{-1}$  indicates a low density of defects and high crystallinity of the graphene.

The tunable passively  $Q$ -switched fiber laser was constructed in a unidirectional ring cavity configuration depicted in Fig. 2. The gain medium was a section of 2

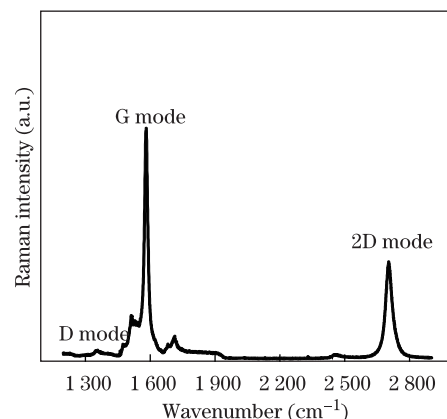


Fig. 1. Raman spectrum of the graphene.

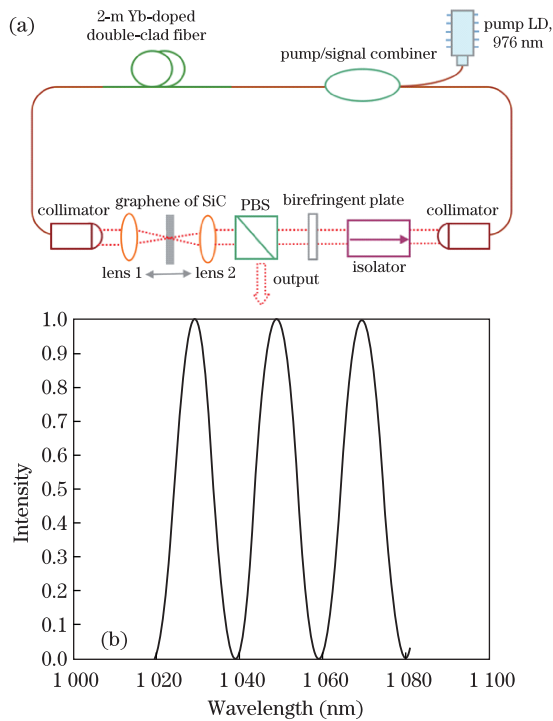


Fig. 2. (a) Experimental setup of the graphene  $Q$ -switched tunable fiber laser. PBS: polarization beam splitter; (b) Transmission curve of the filter.

m Yb-doped single-mode double-clad fiber. The fiber core/inner-cladding diameters were 10/125  $\mu\text{m}$ . Cladding absorption at 976 nm was about 6.5 dB/m. A fiber coupled diode laser with a central wavelength of 975 nm was used as the pump laser. The pump light was coupled into the gain fiber through a pump/signal combiner. Lens 1 was used to focus the laser light onto the graphene-based saturable absorber. The light was then collimated by lens 2. The saturable absorber could be moved between the two lenses, so that the optimum saturable absorption was obtained. The birefringent quartz plate of 4.09-mm thickness, polarization beam splitter (PBS), and the polarization-dependent isolator (ISO) are served as a filter. Figure 2(b) gives the transmission curve of the filter. There are three transmission peak wavelengths within 1020~1080 nm. The bandwidth and the free spectral range around 1050 nm were about 10 and 18 nm, respectively. A remarkable feature of the present fiber laser was that the output light was linearly polarized, which was essential to most laser nonlinear frequency shifting applications, such as frequency doubling and optical parametric oscillation<sup>[30]</sup>. An optical spectrum analyzer (OSA, ADVANTEST, Q8344A) and an oscilloscope (Tektronix, TDS 7104) were used to measure the spectrum and pulse trains of the  $Q$ -switched laser.

Stable  $Q$ -switched pulse train was obtained when pump power increased to 2.24 W. Figure 3(a) shows a typical  $Q$ -switching state of the fiber laser at the pump power of 2.75 W. The repetition rate was 36.6 kHz and the pulse duration was 2.12  $\mu\text{s}$ , which was comparable to the results of graphene  $Q$ -switched fiber lasers reported recently<sup>[10,11]</sup>. The pulse amplitude modulation on the  $Q$ -switched pulse envelope was obvious, which was considered to be the result of self-mode-locking effect. A shorter cavity design along with a narrower bandwidth

filter could reduce the oscillating longitudinal modes which would in turn suppress the self-mode-locking effect<sup>[12]</sup>. Figure 3(b) is the optical spectrum of the  $Q$ -switched pulses. The central wavelength was 1047.41 nm, and the 3-dB bandwidth was 0.88 nm. There were three side peaks at 1030.3, 1052, and 1066.7 nm. Side peaks at 1030.3 and 1066.7 nm agreed with the transmission peak wavelengths of the filter approximately. No specialized technique was used to suppress the mode competition of the gain fiber. The side peaks could be attributed to the graphene-induced nonlinear four-wave-mixing<sup>[17]</sup>, which has been verified to be helpful for multiwavelength generation.

Figure 4 gives the dependence of the repetition rate and the pulse duration against the pump power. When the pump power increased from 2.24 to 4.08 W, the repetition rate grew monotonously. At the pump power of 4.08 W, the repetition rate reached 53.04 kHz. With the increase of the pump power, the pulse duration dropped exponentially from 3.48 to 1.60  $\mu\text{s}$ . When the pump power was higher than 4.08 W, the  $Q$ -switched operation state became unstable. The instability could be attributed to the thermal effect of the graphene considering the fact that when the pump power was increased further, the graphene tended to be damaged.

Figure 5 presents the average output power and pulse energy as a function of the pump power. With the increase of the pump power, the average output power and pulse energy grew monotonically. At the pump power of 4.08 W, the maximum average output power of 35 mW was obtained. The corresponding pulse energy was 0.65  $\mu\text{J}$ . The obtained average power and pulse energy were about 3 and 14 times the results obtained in a graphene  $Q$ -switched Yb-doped fiber laser<sup>[10]</sup>. The higher average power and pulse energy resulted from the use of double-clad gain fiber. The slope efficiency was

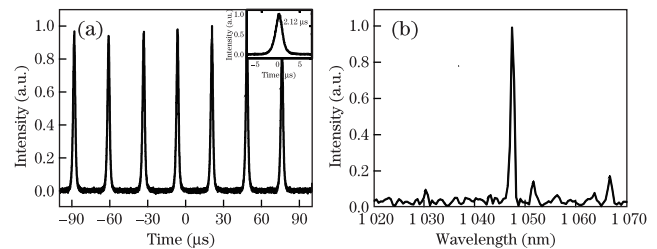


Fig. 3. (a)  $Q$ -switched pulse train and (b) spectrum of the fiber laser. Inset in fig. 3(a) is single pulse.

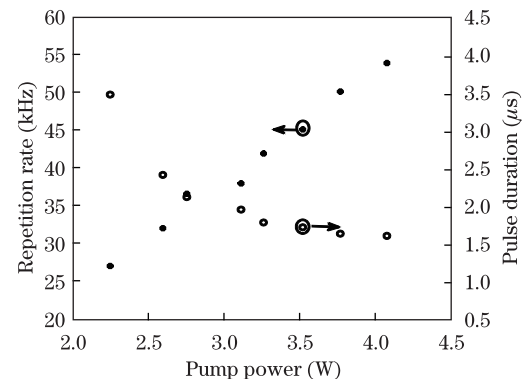


Fig. 4. Pulse repetition rate and pulse duration versus pump power.

about 1.4%. One of the key factors responsible for the low slop efficiency might be the high cavity loss results from the free space section. In addition, the low absorption of the pump light caused by the mismatch between the central wavelength of the pump light and the peak absorption wavelength of the gain fiber was responsible. With further optimization of the laser cavity and the use of wavelength-stabilized pump laser, higher output power and pulse energy could be obtained.

In a passively  $Q$ -switched laser cavity, stable  $Q$ -switching operation usually requires a narrowband lasing optical spectrum to suppress the mode-locking effect, while stable mode-locking operation needs the phase locking among a large number of longitudinal modes. The bandwidth of the filter was about 10 nm, thus mode-locking operation was expected to be achieved in our laser. However, mode-locking was not achieved even with 4.28-W pump power. At higher pump power, the graphene was damaged. A low loss cavity design combined with a polarization controller might be useful for mode-locking operation.

By rotating the quartz plate, spectral tuning of the  $Q$ -switched fiber laser was implemented. Figure 6 gives the spectra of wavelength tunable operation at the pump power of 3.77 W. With the adjustment of the filter, the central wavelength could be continuously tuned from 1038.54 to 1056.22 nm, covering a wavelength range of 17.68 nm. The tuning range was narrower than the gain bandwidth of the Yb-doped fiber, which could be attributed to the narrow free spectral range of the filter. As mentioned above, satellite peaks were obvious due to

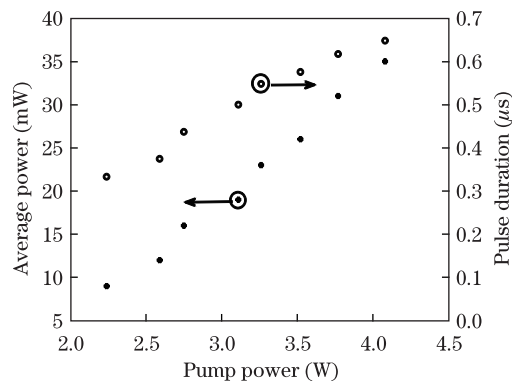


Fig. 5. Average power and pulse energy versus pump power.

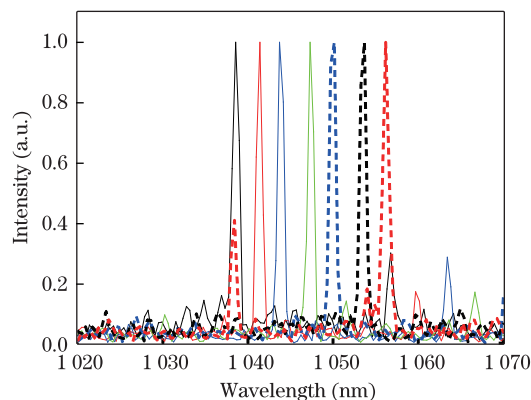


Fig. 6. Spectra of the tunable  $Q$ -switched fiber laser.

the multiple pass bands of the filter. The output power, repetition rate and pulse duration changed slightly over the entire wavelength tuning range.

In conclusion, graphene grown on SiC is successfully used to  $Q$ -switch a Yb-doped double-clad fiber laser. The performance of the pulse repetition rate, pulse width, output power, and pulse energy is investigated. By rotating the quartz filter, the central wavelength of the fiber laser could be continuously tuned from 1038.54 to 1056.22 nm. The double-clad gain fiber enables the fiber laser to deliver  $Q$ -switched pulses with high output power and single pulse energy, and is an encouraging step towards the practical applications of graphene  $Q$ -switched Yb-doped fiber lasers.

This work was supported by the Interdisciplinary Incubation Project Foundation of Shandong University (No. 2011JC025) and Natural Science Foundation of Shandong Province (No. ZR2010FM029).

## References

1. J. A. Alvarez-Chavez, H. L. Offerhaus, J. Nilsson, P. W. Turner, W. A. Clarkson, and D. J. Richardson, *Opt. Lett.* **25**, 37 (2000).
2. S. V. Chernikov, Y. Zhu, J. R. Taylor, and V. P. Gapontsev, *Opt. Lett.* **22**, 298 (1997).
3. W. Zhou, Y. G. Wang, X. H. Li, J. Y. Long, D. Y. Shen, and Y. S. Wang, *Chin. Opt. Lett.* **10(Suppl)**, S21411 (2012).
4. M. Laroche, H. Gilles, S. Girard, N. Passilly, and K. Aït-Ameur, *IEEE Photon. Technol. Lett.* **18**, 764 (2006).
5. J. Y. Huang, H. C. Liang, K. W. Su, and Y. F. Chen, *Opt. Express* **15**, 473 (2007).
6. R. Paschotta, R. Häring, E. Gini, H. Melchior, U. Keller, H. L. Offerhaus, and D. J. Richardson, *Opt. Lett.* **24**, 388 (1999).
7. L. Liu, Z. Zheng, X. Zhao, S. S. Sun, Y. S. Bian, Y. L. Su, J. S. Liu, and J. S. Zhu, *Opt. Commun.* **294**, 267 (2013).
8. W. Zhou, Y. G. Wang, X. H. Li, J. Y. Long, D. Y. Shen, and Y. S. Wang, *Chin. Opt. Lett.* **10(Suppl.)**, S21441(2012).
9. H. Ahmad, F. D. Muhammad, M. Z. Zulkifli, and S. W. Harun, *Chin. Opt. Lett.* **11**, 071401 (2013).
10. J. Liu, S. D. Wu, Q. H. Yang, and P. Wang, *Opt. Lett.* **36**, 4008 (2011).
11. Y. K. Yap, Richard M. De La Rue, C. H. Pua, S. W. Harun, and H. Ahmad, *Chin. Opt. Lett.* **10**, 041405 (2012).
12. L. Wei, D. P. Zhou, H. Y. Fan, and W. K. Liu, *IEEE Photon. Technol. Lett.* **24**, 309 (2012).
13. Z. T. Wang, Y. H. Zou, Y. Chen, M. Wu, C. J. Zhao, H. Zhang, and S. C. Wen, *Laser Phys. Lett.* **10**, 075102 (2013).
14. H. Zhang, D. Y. Tang, R. J. Knize, L. M. Zhao, Q. L. Bao, and K. P. Loh, *Appl. Phys. Lett.* **96**, 111112 (2010).
15. Q. L. Bao, H. Zhang, Y. Wang, Z. H. Ni, Y. L. Yan, Z. X. Shen, K. P. Loh, and D. Y. Tang, *Adv. Funct. Mater.* **19**, 3077 (2009).
16. Z. Q. Luo, M. Zhou, J. Weng, G. M. Huang, H. Y. Xu, C. C. Ye, and Z. P. Cai, *Opt. Lett.* **35**, 3709 (2010).
17. Z. Q. Luo, M. Zhou, D. D. Wu, C. C. Ye, J. Weng, J. Dong, H. Y. Xu, Z. P. Cai, and L. J. Chen, *J. Lightwave Technol.* **29**, 2732 (2011).

18. J. Q. Zhao, P. G. Yan, S. C. Ruan, Y. Q. Yu, G. G. Du, G. L. Zhang, J. Q. Cheng, H. F. Wei, and J. Luo, *Opt. Eng.* **51**, 074201 (2012).
19. L. Q. Zhang, Z. Zhuo, J. X. Wang, and Y. Z. Wang, *Laser Phys.* **22**, 433 (2012).
20. J. Liu, J. Xu, and P. Wang, *Opt. Commun.* **285**, 5319 (2012).
21. C. Liu, C. C. Ye, Z. Q. Luo, H. H. Cheng, D. D. Wu, Y. L. Zheng, Z. Liu, and B. Qu, *Opt. Express* **21**, 204 (2013).
22. B. L. Lu, H. W. Chen, M. Jiang, X. M. Chen, Z. Y. Ren, and J. T. Bai, *Laser Phys.* **23**, 045111 (2013).
23. Z. H. Yu, Y. R. Song, X. Z. Dong, Y. L. Li, J. R. Tian, and Y. G. Wang, *Appl. Opt.* **52**, 7127 (2013).
24. D. Popa, Z. Sun, T. Hasan, F. Torrisi, F. Wang, and A. C. Ferrari, *Appl. Phys. Lett.* **98**, 073106 (2011).
25. D. P. Zhou, L. Wei, and W. K. Liu, *Appl. Opt.* **51**, 2554 (2012).
26. W. Cao, H. Wang, A. Luo, Z. Luo, and W. Xu, *Laser Phys. Lett.* **9**, 54 (2012).
27. H. Ahmad, M. Z. Zulkifli, F. D. Muhammad, A. Z. Zulkifli, and S. W. Harun, *J. Mod. Opt.* **60**, 202 (2013).
28. H. H. Yu, X. F. Chen, H. J. Zhang, X. G. Xu, X. B. Hu, Z. P. Wang, S. D. Zhuang, and M. H. Jiang, *ACS Nano* **4**, 7582 (2010).
29. S. J. Men, Z. J. Liu, X. Y. Zhang, Q. P. Wang, H. B. Shen, F. Bai, L. Gao, X. G. Xu, R. S. Wei, and X. F. Chen, *Laser Phys. Lett.* **10**, 035803 (2013).
30. G. Sobon, J. Sotor, J. Jagiello, R. Kozinski, K. Librant, M. Zdrojek, L. Lipinska, and K. M. Abramski, *Appl. Phys. Lett.* **101**, 241106 (2012).